

# Nullification of Differential Ionospheric Delay for Long-Baseline Real-Time Kinematic Applications

Don Kim and Richard B. Langley

Geodetic Research Laboratory, Department of Geodesy and Geomatics Engineering  
University of New Brunswick, Fredericton, New Brunswick, Canada

## BIOGRAPHY

Don Kim is a research associate in the Department of Geodesy and Geomatics Engineering at the University of New Brunswick (UNB). He has a Bachelor in urban engineering, M.Sc.E. and Ph.D. in geomatics from Seoul National University. He has been involved in GPS research since 1991 and active in the development of an ultrahigh-performance RTK system. He received the Dr. Samuel M. Burka Award for 2003 from the Institute of Navigation.

Richard B. Langley is a professor in the Department of Geodesy and Geomatics Engineering at UNB, where he has been teaching since 1981. He has a B.Sc. in applied physics from the University of Waterloo and a Ph.D. in experimental space science from York University, Toronto. Prof. Langley has been active in the development of GPS error models since the early 1980s and is a contributing editor and columnist for GPS World magazine. He is a fellow of the ION and shared the ION 2003 Burka Award with Don Kim.

## ABSTRACT

One of the major challenges in resolving ambiguities for longer baselines is the presence of unmodelled ionospheric delays. In this paper, we describe a new ionospheric approach that does not rely on the convergence of an ionospheric parameter, and that instantaneously nullifies the effect of the differential ionospheric delay in an ambiguity search process.

The performance of the ionosphere-nullification approach was demonstrated using the data recorded at a 1 Hz data rate at a pair of base stations on either side of the Bay of Fundy in eastern Canada and on the ferry boat, at the

terminals of an approximately 74 km ferry route, on 21 May 2004. The UNB RTK software was enhanced to perform this study. For both static and kinematic tests over the longer 74 km baseline, a few millimeter mean differences were observed in each Cartesian component, and the comparison  $1\sigma$  noise level was at the few centimeter level.

For further enhancements of the UNB RTK software in near future, two issues are discussed in this paper, including a filtering process on the ionosphere observables to reduce the effects of multipath and an estimation of the residual zenith tropospheric delay to remove its residual effects.

## INTRODUCTION

Over the past two years during 2003-2004, the University of New Brunswick (UNB) had carried out a long-term experiment in precise GPS positioning over long distances in a marine environment. The primary goal of the study was to attempt to obtain higher accuracy (centimeter-level) positions at greater distances from differential reference stations. Our approach for achieving high accuracies with GPS technology was real-time kinematic (RTK) data processing in post-processing mode.

Two GPS reference stations had been deployed at the Canadian Coast Guard building in Saint John, New Brunswick (CGSJ) and at the Digby Regional High School in Digby, Nova Scotia (DRHS), on either side of the Bay of Fundy, at the terminals of an approximately 74 km marine ferry route (see Figure 1). Two geodetic-grade receivers (NovAtel's DL-4 receivers and GPS-600 antennas) had been installed at the reference stations. Also, the same type of receiver had been installed on the ferry – the Princess of Acadia. Surface meteorological

equipment had also been collocated with the three receivers. This ferry repeats the same routes between two and four times daily, depending upon the season. The Bay of Fundy is located in a temperate climate with significant

seasonal tropospheric variations (e.g., temperatures between  $-30^{\circ}\text{C}$  and  $+30^{\circ}\text{C}$ ). Data had been collected over the course of one year from the daily ferry runs.

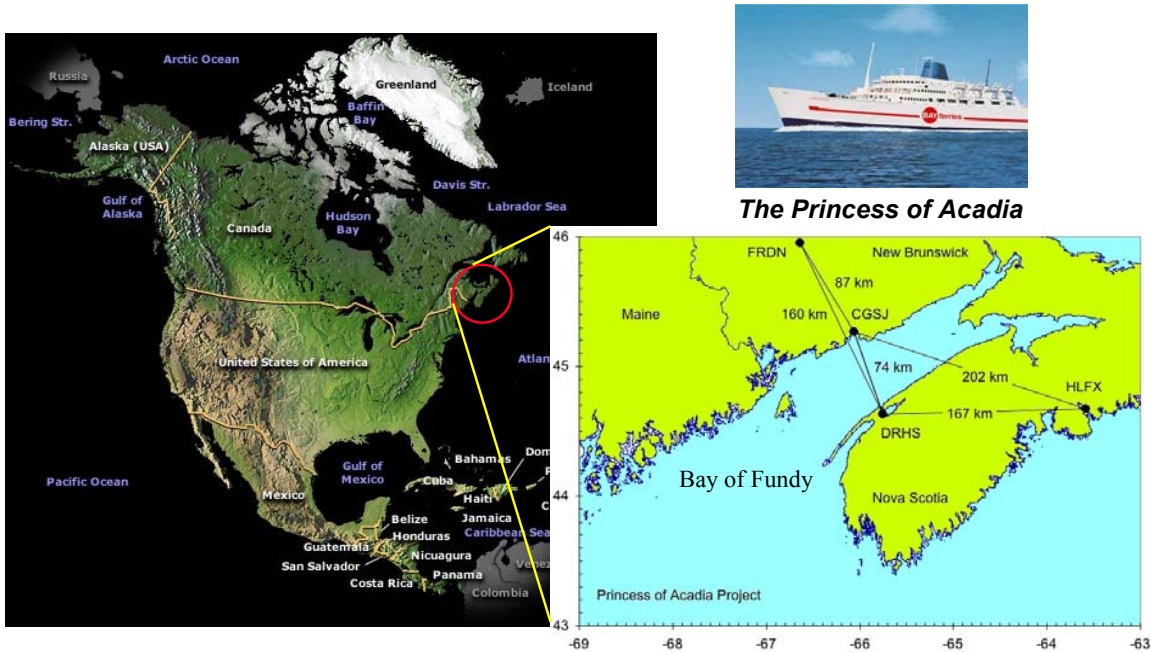


Figure 1. Locale of ferry experiment: Base stations CGSJ and DRHS on either side of the Bay of Fundy –  $\sim 74$  km crossing.

As was reported in Kim et al. [2004], we had attempted to advance positioning results by means of improved differential tropospheric modeling in the study. The differential troposphere experienced by combining GPS measurements from a coastal base station and a near-shore station can differ significantly from land-based baselines. Weather fronts, temperature inversions, and other dynamic coastal weather phenomena degrade the effectiveness of present generic tropospheric delay prediction models [Gregorious and Blewitt, 1998] to the extent that their inability to describe the behavior of the differential troposphere hampers and eventually prevents the successful ambiguity resolution process (which is required in order to obtain cm-level positions) as baselines are lengthened. As the primary limiting factor in successful long-baseline RTK (between 20 and 200 km), we had proposed to improve upon existing tropospheric delay models and tried to integrate these enhancements into the UNB RTK software.

Although we had taken a relatively reliable approach to fixing ambiguities over long distances in the previous study, we had experienced difficulties to some extent in obtaining RTK solutions. Some factors had tended to degrade RTK performance. A typical example was that the number of satellites used for RTK solutions decreased and HRDOP (horizontal relative DOP) and VRDOP (vertical relative DOP) increased as the ferry crosses the

bay. The reason behind this occurrence was unmodelled biases, especially differential ionospheric delay. Since our previous approach did not attempt to remove the differential ionospheric delay in the ambiguity search process, some of the observations were screened out in the quality control routines. As the distance between the reference station and the ferry gets longer, the absolute value of differential ionospheric delay tends to increase. This divergence introduced errors in the observables. Well designed quality control routines can detect growing errors easily and eventually remove the contaminated observations in the RTK processing.

Theoretically, such a divergence in the differential ionospheric delay can be nullified in an ambiguity search process. For example, we can attempt to combine the two independent L1 and L2 ambiguity search processes into one simultaneous ambiguity search process. When a pair of L1 and L2 ambiguity candidates is selected in the simultaneous ambiguity search process, we can completely remove the first-order differential ionospheric delays. In this paper, we investigate the feasibility of this novel approach.

### CONSIDERATIONS FOR A NEW APPROACH

The most common approach for achieving high accuracies with GPS technology is RTK-style processing

– either in real-time or post-processed mode. On designing an appropriate approach for long-baseline RTK, we consider two basic requirements. Firstly, although we process the ferry data in post-processing mode at this stage, our new approach should be based on real-time data processing scenarios for actual implementation in the future. More specifically, we mean single-epoch ambiguity resolution by the real-time data processing scenarios. Secondly, unlike the previous approach used for the ferry data processing [Bisnath et al., 2004], the new approach should provide positioning solutions using fixed ambiguities rather than the ionosphere-free float ambiguities. Previous study using the ionosphere-free float ambiguities produced sub-decimeter solution differences between the long and short baseline position estimates. In this paper, we proceed further by attempting to obtain a few-centimeter positioning results by fixing ambiguities.

One of the tools we use to assess the success of RTK tropospheric and ionospheric models is the comparison between short baseline (e.g., less than a few tens of kilometers) RTK solutions (for which RTK is generally regarded as reliable and uncontaminated by differential atmospheric uncertainties), and simultaneous position solutions from longer RTK baselines over which the tropospheric and ionospheric models are being assessed.

Unfortunately, many RTK systems suffer from reliability problems. These problems include a decrease in system availability with fewer satellites at mid-latitudes ( $\sim 45^\circ$  in this case) or at high-latitudes, susceptibility to biases and errors such as multipath, satellite orbit error, ionospheric refraction and tropospheric refraction.

To improve RTK reliability, we use independent ambiguity resolution for the wide-lane, L1 and L2 observations. As the independently estimated ambiguities must satisfy a constraint (that is, wide-lane ambiguity = L1 ambiguity – L2 ambiguity), we can have an increase in the reliability of the RTK system. This approach has been successfully tested in a gantry crane auto-steering system based on RTK [Kim and Langley, 2003]. Perhaps this approach may not be the best for long-baseline applications in terms of system availability. Furthermore, this approach may not take advantage of dual-frequency observables in canceling the differential ionospheric delay because it will not allow us to use the ionosphere-free linear combination in estimating carrier-phase ambiguities. In this study, however, we tried to overcome this pitfall by developing an algorithm to instantaneously nullify the differential ionospheric delay in the ambiguity search process without introducing the ionosphere-free linear combination.

## IONOSPHERIC DELAYS

In differential GPS, the ionosphere typically has been dealt with in one of three ways: It can be ignored, it can be eliminated using ionosphere-free combinations of dual frequency measurements, or it can be modeled as a state [Richert and El-Sheimy, 2005].

The effect of the differential ionospheric delay is normally negligible when the baseline length to be measured is short. In this case, introducing an ionosphere parameter into the observation equations tends to increase the uncertainty of positioning solutions. In our study, we have ignored the effect of it in processing short baseline (less than a few tens of kilometers) data between one of the reference stations (CGSJ or DRHS) and the ferry. Short baseline RTK solutions have been compared with simultaneous positioning solutions obtained from longer RTK baselines.

Ionosphere-free combinations of data are often used for long baselines because the large residual ionospheric effects are virtually eliminated with this combination. A previous approach applied to the ferry-data processing [Bisnath et al., 2004] had used the ionosphere-free combinations to estimate ionosphere-free float ambiguities. Unfortunately, when ionosphere-free combinations of data are used, the measurement noise is greatly increased. The previous study using these ionosphere-free float ambiguities had produced sub-decimeter solution differences between the long and short baseline position estimates. Furthermore, the solutions had converged quite slowly ( $> 1$  hour) using the ionosphere-free combination.

In general, modeling the ionospheric delays as a state works well for long baselines, and it improves the ability to resolve integer ambiguities. To model the ionospheric delays as a state, an additional parameter for each satellite must be included in the observation equations. This parameter can be estimated using either dual-frequency pseudorange/carrier-phase measurements [Alves et al., 2002] or (in the future) triple-frequency GPS observations [Richert and El-Sheimy, 2005]. In either approach, for a short observation span, the ionospheric delay is highly correlated with the initial carrier-phase ambiguity because both parameters are effectively constant biases, which cannot be separated without a change in geometry. To alleviate this problem, a pseudo-observation, as a constraint on the ionospheric parameter with a certain level of confidence, has been used to improve the convergence of the ionospheric delay. In this case, however, the weighting of this pseudo-observation in the measurement covariance matrix has a significant impact on ambiguity resolution and the accuracy of the final baseline solution. Depending on the weighting factor, the

ionospheric estimates could converge after several tens of minutes or diverge.

## NULLIFICATION OF IONOSPHERIC DELAYS

The ionosphere-free combination and ionosphere modeling work well for long baselines once the parameter (ionospheric delay or float ambiguities) converges. Until now, no one has fully investigated yet another possible approach which does not rely on the convergence of the parameter. Unlike for short baselines, we cannot ignore the effect of the differential ionospheric delay for long baselines. Instead, we can theoretically nullify the effect of the differential ionospheric delay in an ambiguity search process. For example, we can attempt to combine the two independent L1 and L2 ambiguity search processes into one simultaneous ambiguity search process. When a pair of L1 and L2 ambiguity candidates is selected in the simultaneous ambiguity search process, we can virtually eliminate the large residual ionospheric effects (i.e., the first-order differential ionospheric delays). Furthermore, this approach is able to instantaneously eliminate the differential ionospheric delay. We detail the concept of the ionosphere-nullification approach in the following sub-sections.

### The Observation Model

The linearized GPS carrier-phase observation model for long baseline applications is given as:

$$\begin{aligned} \mathbf{y}_i &= \mathbf{A}\mathbf{x} - \mathbf{I}_i + \lambda_i \mathbf{N}_i + \mathbf{m}_i + \mathbf{e}_i, \\ \text{Cov}[\mathbf{e}_i] &= \mathbf{Q}_{y_i}, \quad i = 1 \text{ or } 2, \end{aligned} \quad (1)$$

where  $\mathbf{y}$  is the vector of carrier-phase observations;  $\mathbf{x}$  is the vector of unknown parameters including the baseline components and residual zenith tropospheric delay;  $\mathbf{I}$  is the ionospheric delay parameter where  $\mathbf{I}_2 = (f_{L1}^2 / f_{L2}^2) \mathbf{I}_1$ ;  $\mathbf{A}$  is the design matrix corresponding to  $\mathbf{x}$ ;  $\mathbf{N}$  is the vector of ambiguities;  $f$  and  $\lambda$  are the frequency and wavelength of the carrier-phase observations, respectively; and  $\mathbf{m}$  is the vector of multipath contributions to the carrier-phase observations;  $\mathbf{e}$  is the noise vector including receiver system noise, residual orbit error and residual tropospheric delay;  $\text{Cov}[\cdot]$  represents the variance-covariance operator;  $\mathbf{Q}_y$  is the variance-covariance matrix of the observations; and  $i$  indicates the L1 and L2 signal.

### The Objective Function

Least-squares estimation with integer-constraint for the ambiguity parameters is referred to as an integer least-

squares problem. The objective function to be minimized in the integer least-squares problem,  $\Omega$ , is given as [Euler and Landau, 1992; Teunissen, 1995]:

$$\begin{aligned} \Omega_i &= (\hat{\mathbf{N}}_i - \mathbf{N}_i)^T \mathbf{Q}_{\mathbf{N}_i}^{-1} (\hat{\mathbf{N}}_i - \mathbf{N}_i), \\ \text{with } \mathbf{N}_i &\in \mathbb{Z}^n, \quad i = 1 \text{ or } 2, \end{aligned} \quad (2)$$

where  $\hat{\mathbf{N}}$  is the vector of float ambiguity estimates;  $\mathbf{N}$  is the vector of integer ambiguity candidates selected in the ambiguity search process;  $\mathbf{Q}_{\mathbf{N}}$  is the variance-covariance matrix of the float ambiguity estimates;  $n$  is the number of the observations; and, again,  $i$  indicates the L1 and L2 signal.

### The Ionosphere Observable

The ionospheric delay can be derived from the geometry-free combination once the ambiguity parameters of L1 and L2 are given as known values. The L1 and L2 ionosphere observables are given as:

$$\begin{aligned} \hat{\mathbf{I}}_1 &= \left( \frac{f_{L2}^2}{f_{L1}^2 - f_{L2}^2} \right) [\mathbf{y}_1 - \mathbf{y}_2 - (\lambda_1 \check{\mathbf{N}}_1 - \lambda_2 \check{\mathbf{N}}_2)] \\ \hat{\mathbf{I}}_2 &= \left( \frac{f_{L1}^2}{f_{L2}^2} \right) \hat{\mathbf{I}}_1, \end{aligned} \quad (3)$$

where  $\check{\mathbf{N}}_1$  and  $\check{\mathbf{N}}_2$  are the ambiguity parameters of L1 and L2 as known values, respectively.

### The Nullification Approach

Assuming that a simultaneous search process for L1 and L2 ambiguity parameters has been established, a pair of L1 and L2 ambiguity parameter candidates can be selected in the process. Then, we can derive the L1 and L2 ionospheric observables in Eq. (3) using the ambiguity parameter candidates. As a matter of fact, each ambiguity candidate provides its corresponding ionosphere observable. Once we have a new ionosphere observable, we can estimate a new float ambiguity estimate and its corresponding variance-covariance matrix using Eq. (1). This new float ambiguity estimate and the variance-covariance matrix are free from the effects of the ionospheric delay. We have to carry out the same procedure on each candidate sequentially until no ambiguity candidate remains. Then, our goal is to find the ambiguity candidate that minimizes the objective function in Eq. (2). Figure 2 shows the procedures of the ionosphere-nullification approach.

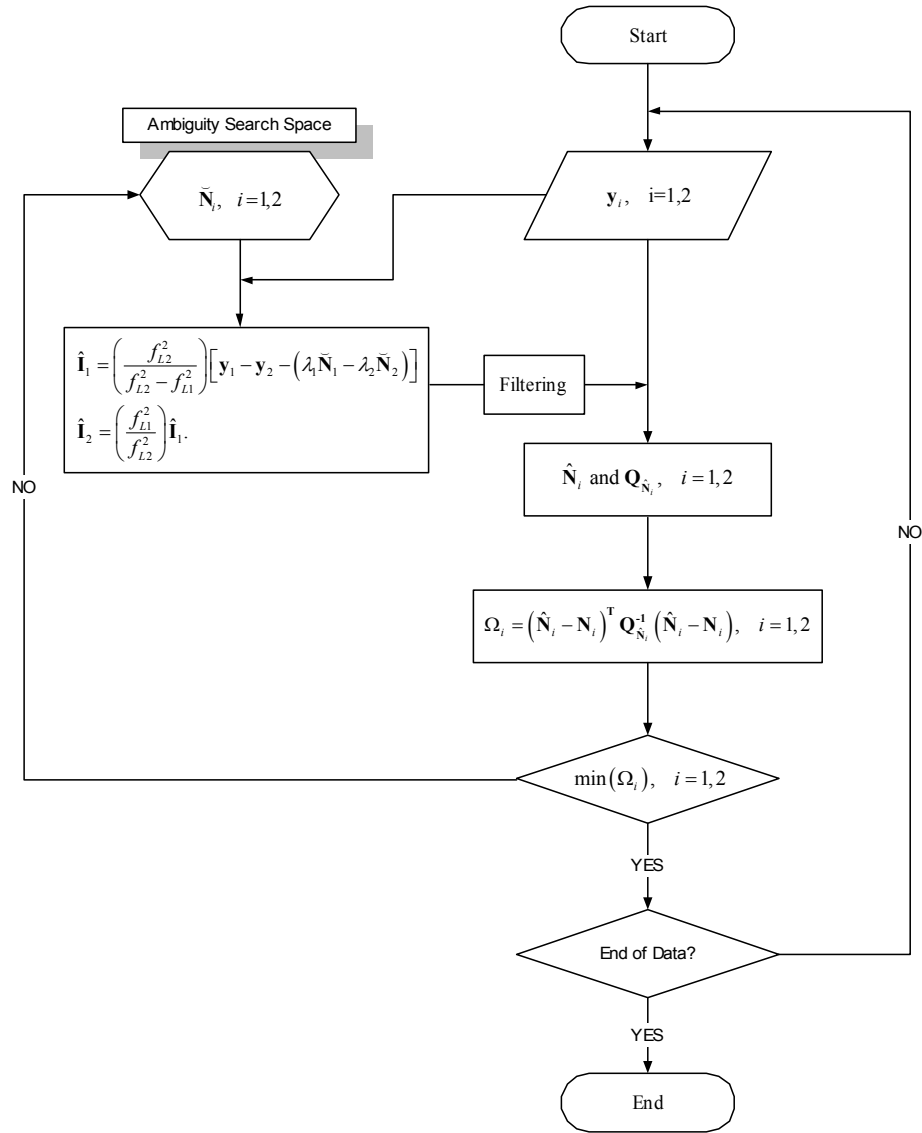


Figure 2. Ionosphere-nullification procedure incorporated in the ambiguity search process.

### Issues in the Nullification Approach

For the purpose of simplicity, we have described conceptual ideas of the ionosphere nullification in the previous sub-section. In fact, the actual implementation of the approach could be to some degree different from the description, depending on the ambiguity search process to be used. Nevertheless, the fundamental ideas are consistent with each other.

One of the issues involved with the ionosphere-nullification approach is the burden of computation. Given  $n$  observations and an ambiguity search range  $W$  for each observation, the total number of ambiguity parameter candidates to be searched turns out to be  $W^{2n}$ . For example, given a  $\pm 1$  m search range (that is,  $W=10$ )

and 9 observations, we will end up with  $10^{18}$  ambiguity candidates. In this case, having a computationally efficient ambiguity search engine is inevitable. UNB's OMEGA (Optimal Method for Estimating GPS Ambiguities) ambiguity search engine finds the first and second best candidates typically in less than 10 ms, using a Pentium 4-M 1.8 GHz IBM Laptop, during one full cycle of data processing, including reading data, decoding observations, searching ambiguities, estimating parameters, and saving parameters and solutions.

Another issue is that the ionosphere observable is apt to be affected by multipath and receiver system noise. Other error sources such as tropospheric delay and satellite orbit error are irrelevant to the observables. From Eq. (3), the noise terms of the ionosphere observables become

$$\begin{aligned} \boldsymbol{\varepsilon}(\hat{\mathbf{I}}_1) &= \left( \frac{f_{L2}^2}{f_{L1}^2 - f_{L2}^2} \right) [\mathbf{e}_1 - \mathbf{e}_2 + \mathbf{m}_1 - \mathbf{m}_2] \\ \boldsymbol{\varepsilon}(\hat{\mathbf{I}}_2) &= \left( \frac{f_{L1}^2}{f_{L2}^2} \right) \boldsymbol{\varepsilon}(\hat{\mathbf{I}}_1). \end{aligned} \quad (4)$$

It should be noted that multipath is normally a dominant error source in the ionosphere observable. Therefore, a GPS antenna should be installed in a clear place with no close-by reflector in the vicinity of the antenna if the ionosphere-nullification approach is to be used in RTK processing. Otherwise, we need to reduce the effects of multipath in the carrier-phase observations when we process the data. The ‘Filtering’ block in Figure 2 can be designed to take care of this issue.

## TEST RESULTS

Using the UNB RTK software, we processed the data recorded at a 1 Hz data rate at a pair of base stations (CGSJ and DRHS) and the ferry boat on 21 May 2004. Since we intended to compare long/short baselines to the same rover to characterize long-baseline positioning performance, we processed a subset of the data near the end of a ferry run that provides such long/short baselines. Figure 3 illustrates the ferry crossing from Digby to Saint John and the data subset used. This situation provided both short (< 3 km) and long (> 73 km) baselines at the same time for one hour.

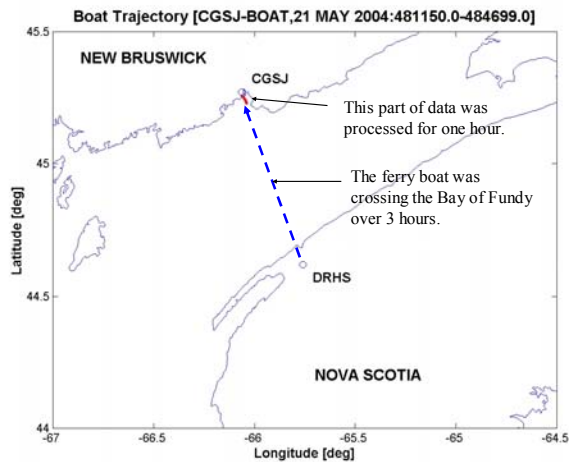


Figure 3. Test data for comparing long/short baselines to the same rover.

## The UNB RTK Software

The UNB RTK software previously mentioned is fundamentally powered by UNB’s OMEGA ambiguity search engine and quality control algorithms. Two

subsidiary tools – an optimal inter-frequency carrier-phase linear combination of the L1 and L2 measurements, and receiver system noise estimation routine – support the system to attain ultrahigh performance GPS positioning and navigation [Kim and Langley, 2003]. The software carries out independent ambiguity resolution for the widelane, L1 and L2 observations to improve RTK positioning reliability. The software processes double-differenced (DD) carrier phase observations in real-time or post-processing mode, in static or kinematic scenarios. Recently, slight modifications have been made to the software to adapt it for long baseline applications. These modifications include troposphere modeling, use of precise orbits and ionosphere nullification.

## NOAA Tropospheric Model

The NOAA tropospheric delay model was developed by the Forecast Systems Lab at the National Oceanic and Atmospheric Administration (NOAA) [Gutman *et al.*, 2003]. The model consists of a numerical weather prediction model in which GPS zenith delay data are assimilated. The GPS data are collected from a large subset of Continuously Operating Reference System (CORS) sites. One manner in which to view this technique is that it allows for the GPS data to constrain the integrated delay in the weather model, while the weather model provides a physics-based method of interpolating and extrapolating delays in space and time. Input parameters are user location and time. Output values are non-hydrostatic (“wet”) and hydrostatic (“dry”) tropospheric delay. Fig. 4 illustrates the zenith wet delay at 1:00 UTC on 21 May 2004. In a previous study on the NOAA experimental tropospheric product, the NOAA zenith total tropospheric delay r.m.s. difference from International GPS Service (IGS) tropospheric estimates ranged from 15 to 25 mm [Bisnath and Dodd, 2004].

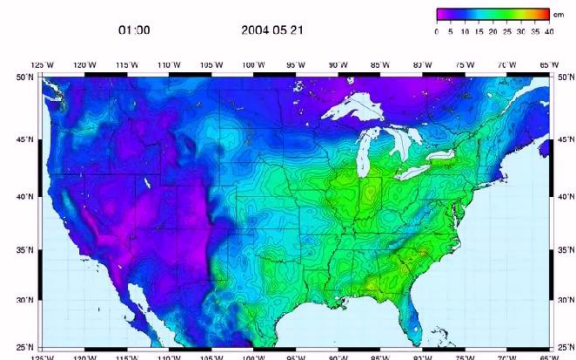


Figure 4. NOAA zenith wet delay at 1:00 UTC on 21 May 2004.

## NGA Precise Satellite Orbit

The National Geospatial-intelligence Agency (NGA) services precise ephemeris files referenced to satellite antenna phase center (APC) rather than center of mass. These files conform to the industry standard SP3 enhanced format. Figure 5 shows an example of double-differenced broadcast orbit errors compared to the NGA APC precise ephemeris for the short and long baselines. These orbit errors were projected onto the range direction.

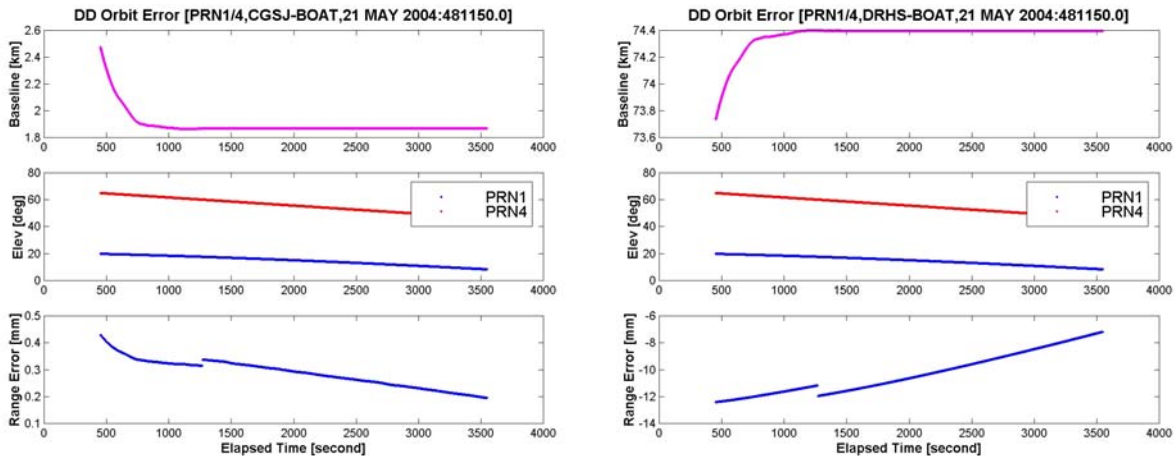


Figure 5. Double-differenced broadcast orbit errors projected onto the range direction: short (left) and long (right) baselines.

## Static Results

A total of three permanent stations already in operation by other organizations have been used to compute the geodetic coordinates of CGSJ and DRHS. One station is located in Fredericton, New Brunswick: the IGS station UNB1, on the Fredericton UNB campus. The other two stations are the U.S. CORS station ESPT, in Eastport, Maine, run by NOAA, and the IGS station HLFX, in Halifax, run by Natural Resources Canada. Seven days of raw GPS data from each reference station were processed with the Bernese V4.2 software [Hugentobler, 2001]. During the processing, the IGS final SP3 orbit product was used and all three permanent station coordinates were held fixed to their ITRF00 coordinates to estimate the coordinates of CGSJ and DRHS. Estimated uncertainty of these coordinates was less than two millimeters.

The first step in the RTK processing to validate the success of the ionosphere-nullification approach was a confirmation of the RTK positioning solutions using the data recorded at CGSJ and DRHS. In this case, although test data was recorded in static mode, the data was processed as if it was obtained in kinematic mode. CGSJ was treated as base station and DRHS as rover.

The top panel shows the distances between one reference station (CGSJ for the short baseline and DRHS for the long one) and the ferry boat, the middle panel shows the elevation angles of the paired satellites used in double differencing, and the bottom panel shows the broadcast orbit errors in the range direction. It is obvious that the effect of broadcast orbit errors is significant for long baselines. Range errors using the broadcast orbit can reach up to a few centimeters.

Figure 6 illustrates that the RTK positioning solutions obtained through the ionosphere-nullification approach agree very well with the reference coordinates of CGSJ and DRHS. On the other hand, the performance of RTK processing without the ionosphere nullification (see the top and bottom panels at the right) was very poor. The reasoning of such a poor RTK performance was a wrong ambiguity resolution as illustrated in Figure 7. In the two bottom panels of the right figure, the L1 and L2 ambiguity parameters were fixed with wrong values at around 750 seconds of elapsed time. We outline the statistics for the ambiguity fixed RTK positioning solutions between CGSJ and DRHS in Table 1.

Table 1. Summary statistics for ambiguity fixed RTK solutions, CGSJ to DRHS on 21 May 2005.

	Mean (cm)	Std. (cm)	r.m.s. (cm)
X	-0.1	1.1	1.1
Y	-0.2	2.3	2.3
Z	-0.3	1.5	1.5
Lat.	0.5	1.4	1.5
Long.	0.6	1.3	1.4
Hgt.	0.4	2.3	2.3

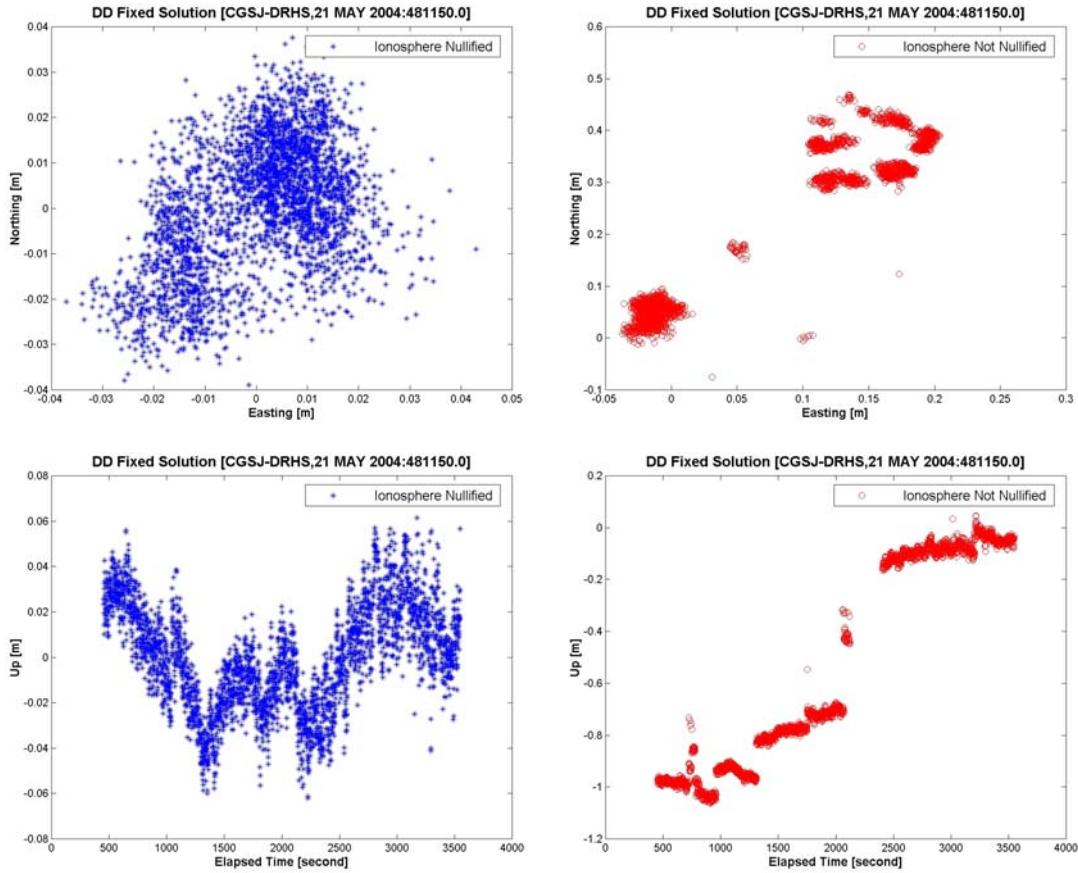


Figure 6. RTK positioning solutions compared with the reference coordinates of CGSJ and DRHS: ionosphere nullification applied (left) and not applied (right).

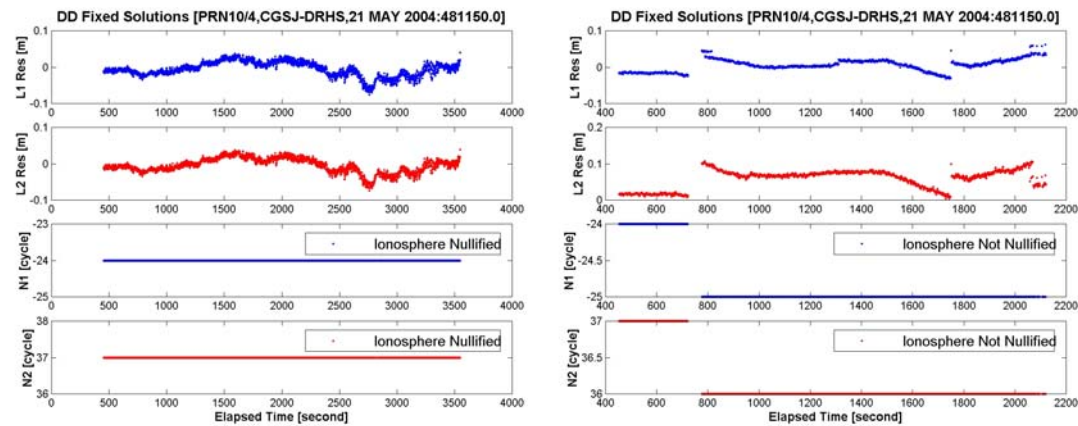


Figure 7. RTK ambiguity resolution and the residuals: ionosphere nullification applied (left) and not applied (right).

Figure 8 shows that the residuals of the L1 and L2 observations are almost identical to those of the ionosphere-free (IF) combinations. This means that the effects of the ionospheric delay have been successfully nullified in the L1 and L2 observations. From Eqs. (1) and (3), the noise terms of the ionosphere-nullified observations becomes

$$\begin{aligned} \boldsymbol{\varepsilon}(\mathbf{y}'_1) &= \boldsymbol{\varepsilon}(\mathbf{y}'_2) = \boldsymbol{\varepsilon}(\mathbf{y}_{IF}) \\ &= \begin{pmatrix} f_{L1}^2 \\ f_{L1}^2 - f_{L2}^2 \end{pmatrix} [\mathbf{m}_1 + \mathbf{e}_1] + \begin{pmatrix} -f_{L2}^2 \\ f_{L1}^2 - f_{L2}^2 \end{pmatrix} [\mathbf{m}_2 + \mathbf{e}_2], \end{aligned} \quad (5)$$

where  $\boldsymbol{\varepsilon}(\mathbf{y}'_1)$  and  $\boldsymbol{\varepsilon}(\mathbf{y}'_2)$  are the noise terms of the ionosphere-nullified L1 and L2 observations,

respectively; and  $\epsilon(y_{IF})$  is the noise terms of the ionosphere-free combination. All three observations have the same noise components in Eq. (5). Note that the ionosphere-nullified L1 and L2 noise terms include multipath contributions from both frequencies. The ‘Filtering’ block in Figure 2 can be designed to reduce multipath contributions to the ionosphere-nullified L1 and L2 observations. We have not yet implemented this function in the current version of the UNB RTK software.

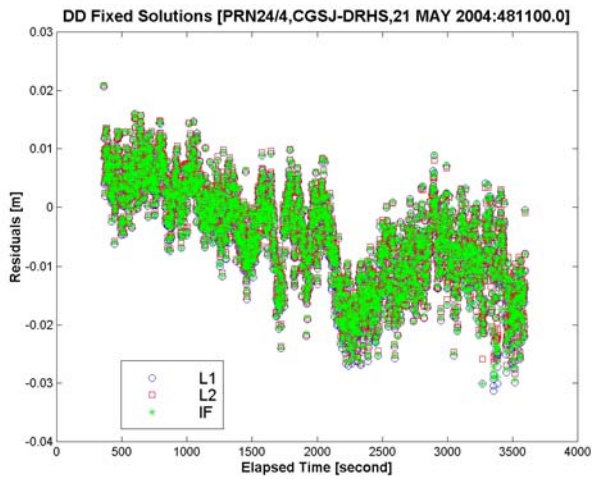


Figure 8. Example of the residuals of least-squares estimation after fixing ambiguities.

For long baselines, multipath, residual orbit error and residual tropospheric delay are the dominant error sources in Eq. (5). Among the error sources, we have seen a significant multipath in the data processed for the study. Figures 9 and 10 illustrate an example of strong multipath in the signal. In Figure 9, the signal from PRN 13 experiences significant multipath at CGSJ while no multipath appears to affect the signal at DRHS. Signal degradation due to multipath is evidenced by the variation

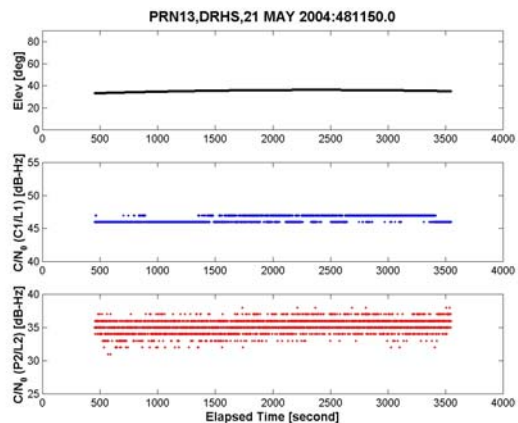
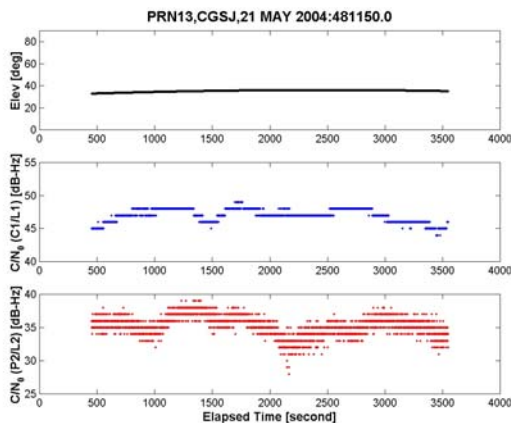


Figure 9. Signal degradation due to multipath (left) and normal (i.e., not problematic) signal reception situations (right), evidenced by the  $C/N_0$  values.

in carrier-to-noise power density ratio ( $C/N_0$ ) values (see the middle and bottom panels at the left). Figure 10 shows the residuals of least-squares estimation after fixing the double-differenced ambiguities of the paired satellites of PRN 13 and PRN 4. The elevation angles of PRN 4 ranged from 50 to 70 degrees and there was no significant signal degradation over the time. Therefore, the pattern in the residuals appears to indicate the presence of multipath in the carrier-phase observations obtained from PRN 13 at CGSJ even if the residual orbit error and the residual tropospheric delay could affect to some degree the residuals. Note that the multipath signature in Figure 10 reflects multipath contributions from both frequencies. As a result, multipath turns out to be one of the limiting factors in our approach in attempting to attain sub-centimeter accuracy for RTK positioning in long baseline situations.

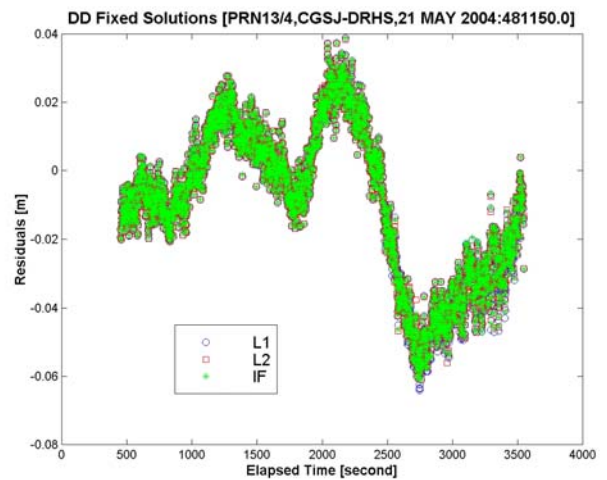


Figure 10. Multipath signature in the residuals of least-squares estimation after fixing ambiguities.

Use of the ionosphere-free combination allows for the estimation of the tropospheric delay when the ambiguity parameters and the baseline components are known. The tropospheric delay observable is given by

$$\hat{\mathbf{T}} = \mathbf{y}_{IF} - \mathbf{A}\hat{\mathbf{x}} - \left( \frac{f_{L1}^2}{f_{L1}^2 - f_{L2}^2} \right) \lambda_1 \tilde{\mathbf{N}}_1 + \left( \frac{f_{L2}^2}{f_{L1}^2 - f_{L2}^2} \right) \lambda_2 \tilde{\mathbf{N}}_2. \quad (6)$$

Note that Eq. (6) assumes no orbit error and multipath, and so is a crude approximation of the tropospheric delay. Figure 11 illustrates that the residual tropospheric delay is another limiting factor in attempting to attain sub-

centimeter accuracy of RTK positioning for long baselines. The residuals of the least-squares estimation after fixing ambiguities (left) reflects exactly the trend of the residual tropospheric delay (that is, the difference between the tropospheric delay observable in Eq. (6) and the NOAA prediction model) in the bottom panel (right). In this case, the RTK positioning can be improved if the residual zenith tropospheric delay is estimated as an unknown parameter in Eq. (1). We have not yet implemented this in the present version of the UNB RTK software.

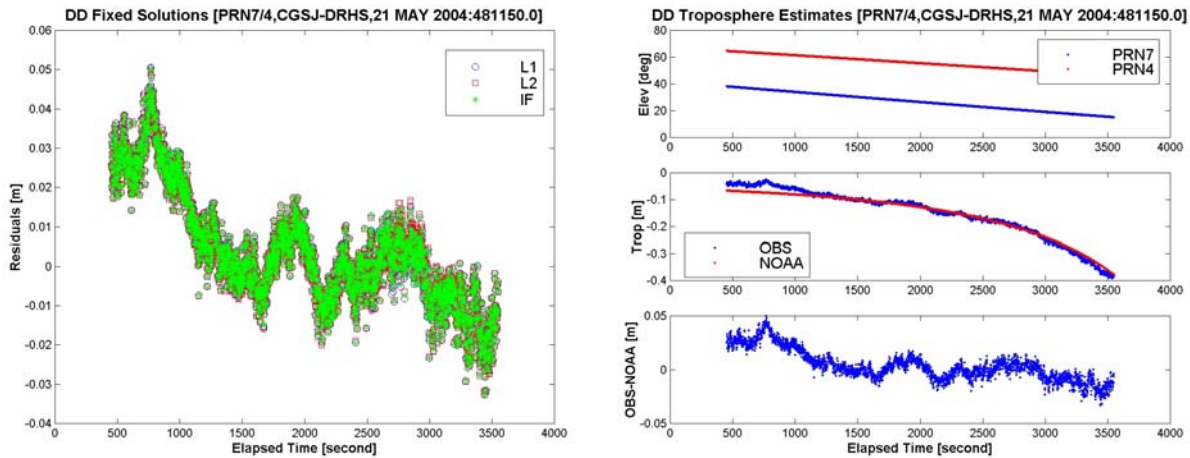


Figure 11. The residuals of least-squares estimation after fixing ambiguities (left) and the residual tropospheric delays of the NOAA prediction model (right).

### Kinematic Results

Since we have validated the success of the ionosphere-nullification approach using the data recorded in static mode at CGSJ and DRHS, we further tried to confirm its validity using the data collected in kinematic mode with the onboard GPS receiver. A pair of long/short baselines (i.e., DRHS to BOAT and CGSJ to BOAT) was estimated at each epoch and used to characterize long-baseline positioning performance. The same procedures as mentioned in the previous section ‘Static Results’ were applied for long baseline RTK processing.

For short baselines, the ionosphere-nullification approach was not applied since it tends to increase the noise and eventually the uncertainty of positioning solutions as illustrated in Figure 12. The residuals of L1 and L2 observations in the right figure (i.e., the case of ionosphere nullification not applied) are less noisy than those of the left figure (i.e., the case of ionosphere nullification applied).

From the residual analysis, we have seen significant effects of multipath in the carrier-phase observations. The funnel of the ferry boat in Figure 13 might be one of the signal reflectors generating such a strong multipath. Since multipath is one of the limiting factors in our approach in attempting to attain sub-centimeter accuracy of RTK positioning for long baselines, the onboard GPS antenna should have been located in a better place. Nevertheless, we will try to develop the filtering process in Figure 2 in the near future to reduce the effects of multipath in the carrier-phase observations when we process the data.



Figure 13. Onboard GPS antenna under multipath rich environment.

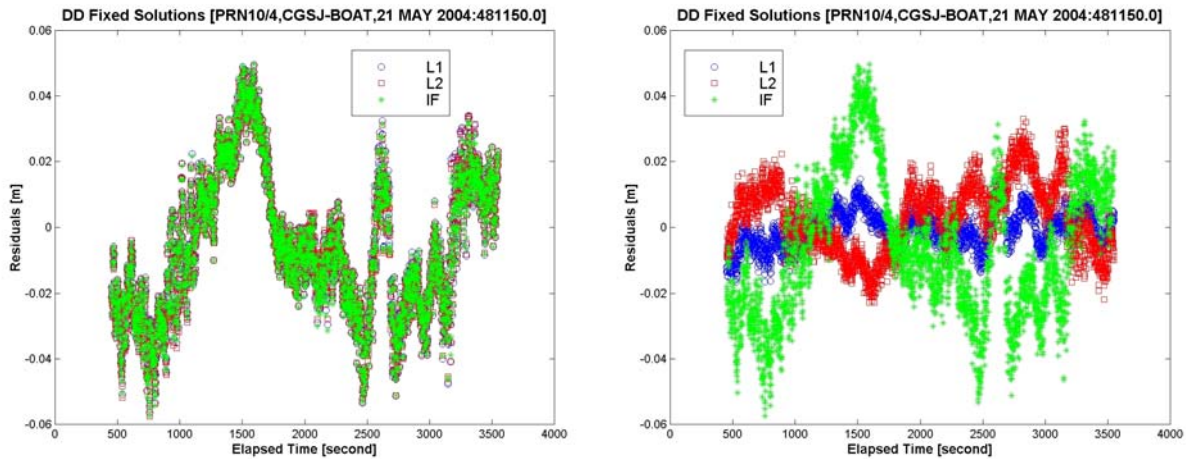


Figure 12. The residuals of least-squares estimation after fixing ambiguities: the ionosphere nullification was applied (left) and not applied (right).

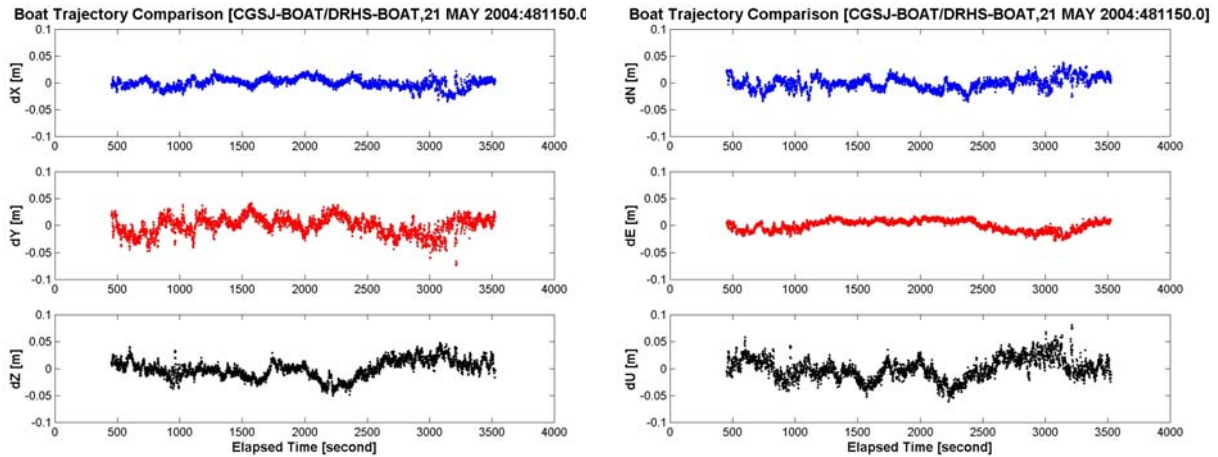


Figure 14. Difference of RTK positioning solutions, CGSJ to BOAT (short baseline) and DRHS to BOAT (long baseline) in Cartesian (left) and local geodetic coordinates (right).

Table 2. Summary statistics for difference between ambiguity fixed RTK solutions: CGSJ to BOAT and DRHS to BOAT on 21 May 2005.

	Mean (cm)	Std. (cm)	r.m.s. (cm)
X	-0.1	0.9	0.9
Y	-0.2	1.7	1.7
Z	-0.3	1.6	1.6
Lat.	-0.3	1.2	1.2
Long.	-0.2	1.0	1.0
Hgt	-0.1	2.0	2.0

Figure 14 illustrates that there is only few centimeter noise variation between the long and short RTK positioning solutions. Table 2 summarizes the statistics. A few millimeter mean differences are observed in each

Cartesian component, and the comparison  $1\sigma$  noise level is at the few centimeter level.

## CONCLUSIONS AND FUTURE WORK

One of the major challenges in resolving ambiguities for longer baselines is the presence of unmodelled ionospheric delays.

Ionosphere-free combinations of data have been used for longer baselines because the large residual ionospheric effects are virtually eliminated with this combination. When ionosphere-free combinations of data are used, however, the measurement noise is greatly increased and the solutions tend to converge quite slowly.

Modeling the ionospheric delays as a state also works well for long baselines. As a constraint on the ionospheric parameter with a certain level of confidence, a pseudo-observation has been used to improve the convergence of the ionospheric delay. However, the weighting of this pseudo-observation in the measurement covariance matrix has a significant impact on ambiguity resolution and the accuracy of the final baseline solution. Depending on the weighting factor, the ionospheric estimates could converge after several tens of minutes or diverge.

In this paper, we investigated another possible approach that does not rely on the convergence of the parameter, and that nullifies the effect of the differential ionospheric delay in an ambiguity search process. For example, we can attempt to combine the two independent L1 and L2 ambiguity search processes into one simultaneous ambiguity search process. When a pair of L1 and L2 ambiguity candidates is selected in the simultaneous ambiguity search process, we can virtually eliminate the large residual ionospheric effects using the ionosphere observable. Furthermore, this approach is able to instantaneously eliminate the differential ionospheric delay.

We demonstrated the performance of the ionosphere-nullification approach using the data recorded at a 1 Hz data rate at a pair of base stations and on a ferry boat. For both static and kinematic tests over a 74 km baseline, a few millimeter mean differences are observed in each Cartesian component, and the comparison  $1\sigma$  noise level is at the few centimeter level.

Multipath and the residual tropospheric delay turned out to be the most significant limiting factors in our approach in attempting to attain sub-centimeter accuracy RTK positioning for long baselines. Further enhancements of the UNB RTK software will be made in near future with respect to the following two issues:

- Filtering process on the ionosphere observables contaminated by multipath.
- Estimation of the residual zenith tropospheric delay.

## ACKNOWLEDGEMENTS

The authors would like to thank the U.S. Office of Naval Research for funding this research during 2003-2004 through an agreement with the University of Southern Mississippi. Thanks also goes to the Canadian Coast Guard, Marine Atlantic (and crew of the Princess of Acadia), and Digby Regional High School for hosting GPS/meteorological stations.

## REFERENCES

- Alves, P., G. Lachapelle, M. E. Cannon, J. Park, and P. Park (2002). "Use of self-contained ionospheric modeling to enhance long baseline multiple reference station RTK positioning" Proceedings of ION GPS 2002, 15th International Technical Meeting of the Satellite Division of The Institute of Navigation, Portland, Oregon, September 24-27, 2002; pp. 1388-1399.
- Bisnath, S., D. Wells, M. Santos, and K. Cove (2004). "Initial results from a long baseline, kinematic, differential GPS carrier phase experiment in a marine environment." Presented at IEEE PLANS 2004, Monterey, California, 26-29 April.
- Bisnath, S. and D. Dodd (2004). "Analysis of the utility of NOAA-generated tropospheric refraction corrections for the next generation nationwide DGPS service." Proceedings of ION GNSS 2004, 17th International Technical Meeting of the Satellite Division of The Institute of Navigation, Long Beach, CA, 21-24 September 2004; pp. 1288-1297.
- Euler, H.-J. and H. Landau (1992). "Fast GPS ambiguity resolution on-the-fly for real-time application." Proceedings of Sixth International Geodetic Symposium on Satellite Positioning, Columbus, Ohio, 17-20 March; pp. 650-659.
- Gregorius, T. and G. Blewitt (1998). "The effect of weather fronts on GPS measurements." GPS World, Vol. 9, No. 5; pp. 53-60.
- Gutman, S.I., T. Fuller-Rowell, and D. Robinson (2003). "Using NOAA atmospheric models to improve ionospheric and tropospheric corrections." Presentation to U.S. Coast Guard DGPS Symposium, 17-19 June, Portsmouth, Virginia.
- Hugentobler, U., S. Schaer and P. Fridez (2001) Bernese GPS Software Version 4.2, Astronomical Institute, University of Berne, Switzerland.
- Kim, D. and R. B. Langley (2003). "On ultrahigh-precision positioning and navigation." Navigation: Journal of the Institute of Navigation, Vol. 50, No. 2, Summer; pp. 103-116.
- Kim, D., S. Bisnath, R. B. Langley and P. Dare (2004). "Performance of long-baseline real-time kinematic applications by improving tropospheric delay modeling." Proceedings of ION GNSS 2004, 17th International Technical Meeting of the Satellite Division of The Institute of Navigation, Long Beach, CA, 21-24 September 2004; pp. 1414-1422.
- Richert, T. and N. El-Sheimy (2005). "Ionospheric modeling: The key to GNSS ambiguity resolution." GPS World. Vol. 16, No. 6; pp. 35-40.
- Teunissen, P. J. G. (1995). "The least-squares ambiguity decorrelation adjustment: A method for fast GPS integer ambiguity estimation." Journal of Geodesy, Vol. 70, No. 1-2; pp. 486-501.